Available online at www.sciencedirect.com
SCIENCE DIRECT®
PERGAMON
Materials Science in Semiconductor Processing 5 (2003) 199–206
MATERIALS SCIENCE IN SEMICONDUCTOR PROCESSING

Phase transformation and paired-plate precipitate formation in $Pb_{0.91}La_{0.09}Zr_{0.65}Ti_{0.35}O_3$ films grown on sapphire substrates

B. Tunaboylu[a], C.S. Ozkan[b,*], A. Ata[c], K. Ring[d], S. Esener[d]

[a] *Kulicke and Soffa Inc., Gilbert, AZ, 85233, USA*
[b] *Mechanical Engineering Department, University of California, Riverside, CA 92521, USA*
[c] *Department of Materials Science, Gebze Institute of Technology, Gebze 41400 Kocaeli, Turkey*
[d] *Electrical and Computer Engineering Department, University of California, San Diego, CA, 92037, USA*

Abstract

We report on the phase transformation behavior of $Pb_{0.91}La_{0.09}Zr_{0.65}Ti_{0.35}O_3$ (9/65/35) PLZT films grown on r-sapphire substrates via rf-magnetron sputtering. A complex microstructure results in these films depending on deposition and annealing conditions. A random equiaxed polycrystalline grain morphology was observed after rapid thermal annealing or furnace annealing when the as-deposited films were predominantly pyrochlore. Precipitate formation (100–150 nm) was observed in PLZT films that were deposited at temperatures in excess of 490°C with a perovskite structure, after furnace annealing at 700°C. We believe that this is related to internal stresses in the films due to both the lattice mismatch and the thermal expansion mismatch between the PLZT film and the sapphire substrate.
© 2002 Elsevier Science Ltd. All rights reserved.

Keywords: Ferroelectrics; PLZT; Precipitate splitting; Magnetron sputtering

1. Introduction

Ferroelectric lead lanthanum zirconate titanate (PLZT) films deposited by various techniques are typically amorphous or a mixture of crystalline pyrochlore and perovskite phases. Post-deposition annealing is necessary to transform the film into desired perovskite phase to improve the electrical and electro-optic properties for many deposition processes, such as metal-organic decomposition, sol–gel processing, laser ablation or sputtering. An intermediate phase(s), usually pyrochlore ($La_2Zr_2O_7$) forms at deposition temperatures. This phase is non-ferroelectric and has very low dielectric constant, and transforms to the perovskite phase fully or partially at higher annealing temperatures, >600°C. Pyrochlore is reported to be present as an intermediate phase between 300–600°C, and transforms to perovskite at higher temperatures [1,2]. The PLZT 9/65/35 shows very large electro-optic coefficients, making it attractive for electro-optic applications such as spatial light modulators, waveguide modulators, and optical switches [1]. Isothermal transformation kinetics of amorphous to perovskite phase of powder PLZT 8/65/35 from nitrate solutions has been studied [3] and it was inferred from the experimental data that nucleation of perovskite from amorphous powders was the rate limiting step. The activation energy of crystallization of these powders was found to be 297 kJ/mol. The activation energy for the pyrochlore–perovskite phase transformation in PLZT 9/65/35 films was determined to be 322 ± 48 kJ/mol, which showed a $t^{1/2}$ dependence as a function of the heat treatment temperature and indicated a diffusion controlled transformation [4].

Solid state phase transformations are known to often generate coherent second phase precipitates. Particle shape transitions occur with a coherent precipitate increasing its size during either coarsening or growth stages. Sphere to cube and cube to cuboid or ellipsoid shape transitions are among the common

*Corresponding author. Tel.: +1-909-787-5016; fax: +1-909-787-2899.
E-mail address: cozkan@engr.ucr.edu (C.S. Ozkan).

1369-8001/02/$ - see front matter © 2002 Elsevier Science Ltd. All rights reserved.
PII: S1369-8001(02)00073-2

transformations. Precipitates are spherical when they are small initially and they become cuboidal as their size increases. In exception to this trend, some cuboid particles were observed to evolve into plate-shaped particles that split or fission into two (or more) smaller particles. This different type of transition, splitting of cuboid into two parallel plate-like smaller particles, is termed as *precipitate splitting*. Precipitate pair formation or precipitate splitting has been reported previously in Ni-based super alloys [5–7]. The splitting and coarsening process in such alloys have received a great deal of attention from researchers due to the formation and evolution of a variety of complex morphology of precipitate particles in a parent matrix because of their impact on material properties. Theoretical analyses generally agree that particle splitting is related to the existence of internal stress in two-phase systems with significant lattice mismatch and low interfacial energy density. The balance between the interfacial energy and the elastic energy is an important determinant of the morphology and splitting. In this work, we present the formation of paired plate precipitate structures in PLZT (9/65/35) films on r-plane sapphire substrates. We have previously analyzed PLZT (9/65/35) films on Pt/Si substrates and have not observed any microstructure revealing precipitate splitting [9]. Similarly, no such precipitate structures but 200 nm crystallites of random orientation have been reported on PLZT (9/65/35) on c-sapphire [13] or films of other PLZT compositions on silicon [11]. Grains of various sizes and clusters of crystallites surrounding a fine grained matrix were observed for acetate-derived PLZT (9/65/35) films on SnO_2 coated PLZT plates, polycrystalline Al_2O_3 and single crystal sapphire substrates [17]. Paired plated formation observed on this study on PLZT (9/65/35) films on r-sapphire substrates have not been reported previously for any ferroelectric films. It appears that the type of substrate has played an instrumental role in their formation.

2. PLZT film deposition

PLZT 9/65/35 films were deposited on r-plane sapphire substrates using an off-axis rf-triode magnetron sputtering system. The basic elements of this system are a thermal-electron emitting filament, an anode, a plasma-confining enclosure and a sputtering target. The filament is heated by a high-current AC power supply to a temperature sufficient for thermal electrons to boil off its surface, set to 36 A in our experiments. These electrons are then attracted to an anode biased positively by a high-voltage DC power supply. Gas atoms, argon in this case, bled into the enclosure where they collide with the accelerated electrons generating ions and thus a self-sustaining arc-type plasma will be initiated. Typically, this electron-enhanced plasma will be sustained at voltages of 50–70 V and at currents up to 10 A. To initiate the sputtering process, a negative voltage DC or RF bias supply is applied to the target and plasma ions are attracted and accelerated towards the target surface. Low pressures reduce the amount of gas atoms embedded in the films, improving the film density. Magnetic fields trap electrons emitted from cathode as an orbit around the field lines and electrons undergo a drift motion in the direction perpendicular to both the electric and the magnetic fields. These electrons make large number of collisions, thus producing an intense plasma discharge.

PLZT sputtering targets with nominal 9/65/35 composition manufactured by Balzers Materials (Hudson, NH, USA) were used. The target was bonded to a copper backing-plate using a conductive silver epoxy at room temperature. PLZT deposition was conducted at temperatures from 250°C to 490°C through backside lamp heating and using argon as at a pressure of 0.5 Pa. Low pressure sputtering combined with substrate rotation have resulted in very good film thickness uniformity.

3. Post deposition annealing and film characterization

Post deposition annealing was carried out via rapid thermal annealing in N_2 or N_2/O_2 environment or furnace annealing in O_2 environment. The RTA processor used in this study included a 2.54 cm (1″) quartz tube surrounded by banks of tungsten halogen lamps for fast heating. The thin-film sample was placed on a 25 mm × 13 mm graphite (or quartz) plate holder with 1 mm walls on top to contain the sample and the silicon wafer underneath. A chromel–alumel thermocouple was extended through an quartz encasing tube to be in contact with the back of silicon wafer to monitor the temperature. In our experiments, the graphite holder was observed to be more consistent in temperature readings, using independent thermocouples, than a quartz holder probably due to much higher absorptivity of graphite. Furnace annealing was carried out in 2.54 cm (1″) quartz tubes in oxygen with PbO ambient provided by PLZT ceramic of the same composition with excess PbO located near the thin-film sample.

Microstructure of the films were characterized using scanning electron microscopy (SEM) and transmission electron microscopy (TEM). SEM was used to image different film morphologies and initial characterization. TEM work was performed on samples carefully prepared by dimpling and ion milling to obtain some transparent sections of mechanically cut 3 mm disks. These disks were at first ground to 100 μm and then dimpled to 25 μm and subsequently ion milled at an angle of 10° using double 5 kV argon beams to final

transparent thickness. Rutherford backscattering spectrometry (RBS) was conducted to characterize the as-deposited and annealed film compositions. X-ray diffraction (XRD) was conducted to determine the crystal structure of the films.

4. Results and discussion

4.1. Film composition and crystal structure

The sputtered film composition as a function of substrate temperature is shown in Fig. 1. The volatility of Pb was significant during PLZT sputter deposition as observed from the plot. Lead depletion at very low temperatures is probably due to the geometry of the system as well as the type of sputter sources selected for deposition. The large source to substrate distance contributed to the low arrival rates of Pb as well as causing lower deposition rates. However, the choice was useful in obtaining films with good uniformity. It should be noted that two multi-component hot-pressed and compensated PLZT targets were used that contained 20 and 30 at% excess PbO. The Zr/Ti atomic ratio was relatively constant in the substrate temperature regime. The sputtering gas was 100% inert argon and no oxygen was added as the reactive ambient caused compositional shifts in the target as well as on the films. The films deposited at temperatures between 300°C and 450°C showed excess Pb content and loss of Pb/PbO was noticeable above 450°C, and depleted dramatically at 600°C. The excess Pb in the films deposited at low substrate temperatures in the range 6% Pb excess to 29% Pb excess was confirmed by RBS. Fig. 2 shows a stoichiometric PLZT 9/65/35 film on sapphire which was obtained at temperatures just below 500°C and rapid thermally annealed at 700°C for 3 min. RBS spectrum of a furnace annealed (700°C, 1 h) stoichiometric PLZT 9/65/35 film on r-sapphire is illustrated in Fig. 3.

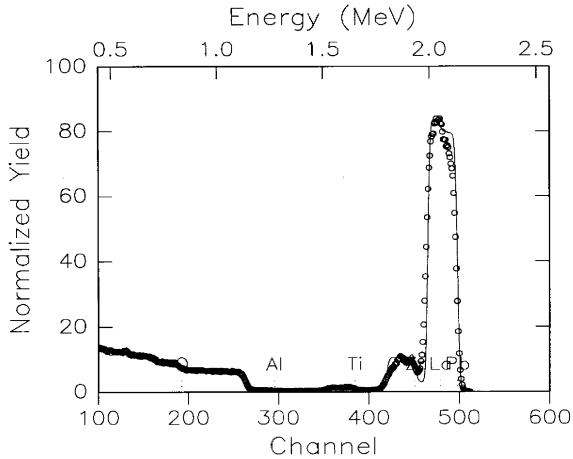

Fig. 2. RBS spectrum of stoichiometric PLZT 9/65/35 film on sapphire. The post-RTA film thickness is 0.44 μm.

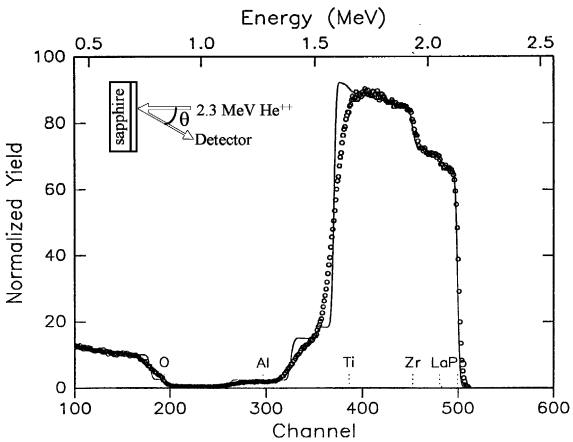

Fig. 3. RBS spectrum of stoichiometric PLZT 9/65/35 film grown on sapphire (700°C for 1 h).

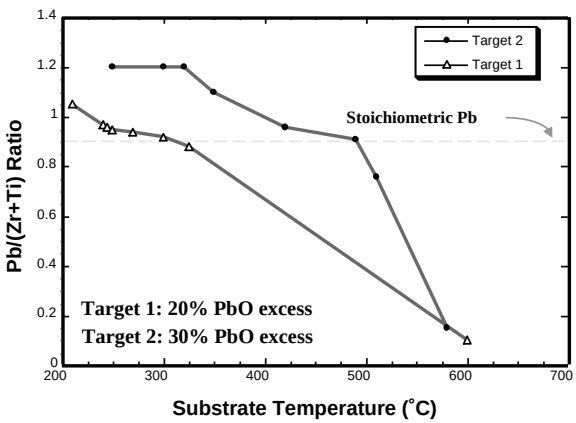

Fig. 1. Film lead content as a function of substrate temperature using hot-pressed single PLZT oxide targets with excess PbO.

Crystal structures formed in the as-deposited or annealed films were determined by X-ray diffraction. PLZT films deposited on sapphire at substrate temperatures below 300°C showed an amorphous phase (Fig. 4) which crystallized into the perovskite phase after RTA processing at 730°C for 3 min, as shown in Fig. 5 for deposition temperatures of (a) 245°C, (b) 250°C and (b) 260°C. The peak denoted as 'o' belongs to pyrochlore. It is interesting to note that the PLZT films were oriented in (1 1 0) direction and they had tetragonal lattice structure since both (1 0 1) and (1 1 0) reflections were present. The tetragonal distortion from cubic lattice was very small and the calculated lattice constants were a = 0.4086 nm and c = 0.4109 nm. It is possible to

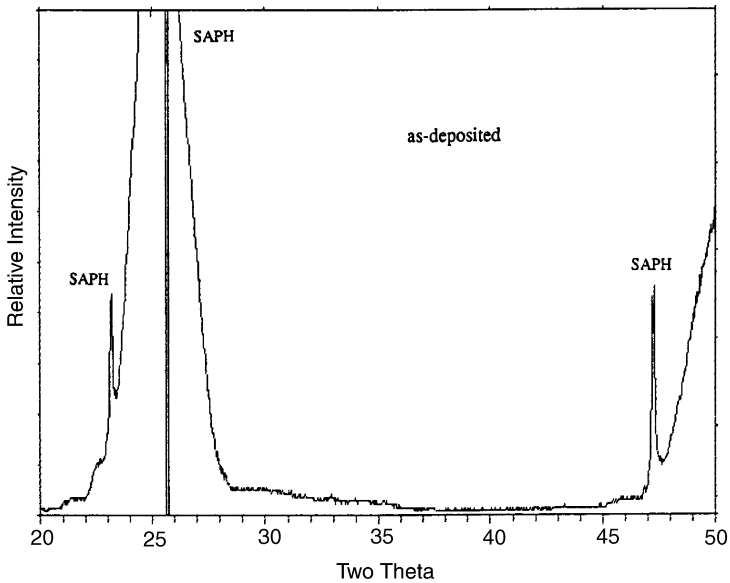

Fig. 4. X-ray diffraction pattern of as-deposited PLZT thin film on sapphire indicating an amorphous phase.

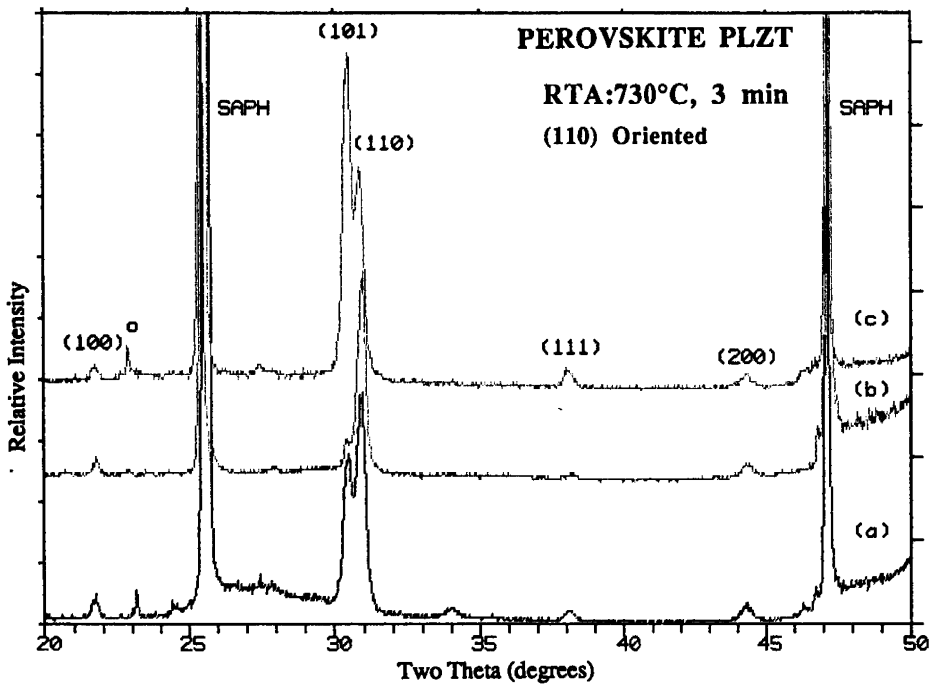

Fig. 5. XRD patterns of PLZT/sapphire showing the perovskite phase (indexed) after RTA treatment at 730°C for 3 min.

circumvent the formation of pyrochlore by rapid thermal annealing which also yielded transparent films with smooth surfaces. The films had (1 1 0) orientation and the degree of orientation (PO) was 96% and 88% for the films annealed at 730°C and 700°C, respectively. The PO(1 1 0) was estimated from the integrated intensities ($I^{(hkl)}$) of (1 1 0) and (1 0 0) reflections, using the equation $PO = I^{(1\,1\,0)}/(I^{(1\,1\,0)} + I^{(1\,0\,0)})$. The PLZT films

had nearly all perovskite phase after 3 min RTA cycle at 730°C, however there is a residual pyrochlore phase after RTA treatment at 700°C. It was found that Pb-stoichiometry is maintained at both of these RTA temperatures.

The annealing atmosphere for RTA was N_2 or N_2/O_2. There was no appreciable difference in the phase transformation behavior of PLZT films processed in either rapid thermal annealing atmosphere. However, the atmosphere was pure oxygen to ensure full phase transformation to perovskite phase in films in the furnace annealing case. To enhance perovskite crystallization and retain a stoichiometric PLZT film, a Pb ambient environment above the film during furnace annealing was found to be necessary. Otherwise, furnace annealed films were Pb-deficient and retained a pyrochlore phase which was not fully transformed to perovskite. The air ambient was not as effective as O_2 environment for perovskite formation in furnace annealing.

4.2. Microstructure characterization of as-grown and annealed films

A polycrystalline pyrochlore phase forms at low deposition temperatures, >300°C, and usually coexists with an amorphous phase. Such a PLZT (9/65/35) film with nano-crystals of pyrochlore islands in an amorphous matrix is seen in Fig. 6. Perovskite phase forms and coexists with pyrochlore phase at higher deposition temperatures and the film transforms to fully perovskite at very high deposition temperatures above 490°C. Annealing is often needed to convert any trace amounts of a second phase into the perovskite phase to obtain better electrical and electro-optical performance. PLZT films can be heat-treated either by RTA or furnace annealing to obtain a single-phase. However, a slow cooling procedure must be adopted in the RTA to prevent micro-cracking in the films due to excessive thermal stresses.

Fig. 7(a) shows a SEM micrograph illustrating a microstructure consisting of pockets of round pyrochlore grains in an amorphous matrix of a PLZT film after RTA at 550°C for 2 min. Some of the denser areas of these pyrochlore clusters form perovskite phase at higher annealing temperatures. The final microstructure shows a uniform matrix of grains of approximately 300 nm (Fig. 7(b)). Furnace annealed films generally exhibit larger equiaxed grain sizes of approximately 1000 nm. A representative microstructure common to PLZT films deposited below 450°C and furnace annealed at 700°C for 30 min is presented in Fig. 7(c).

We used a direct measurement of temperature using thermocouples, instead of pyrometers that require data on optical properties of the wafer and the quartz tube to calibrate the temperature. It should be noted that the total error in measured steady-state temperatures from both the thermocouple junctions and the measurement apparatus was estimated to not to exceed ± 5°C, including the error due to heat loss from the wafer to the thermocouple. One precaution taken in our RTA tests was that two cycles were necessary for the process to reach a quasi-steady-state condition before the actual test runs. Because of its lower absorptivity and greater thermal mass, the quartz chamber is heated at a slower rate than the wafer sample piece itself as suggested by other workers [7]. Simulations done for similar chamber geometry and sample configuration [8] show that the

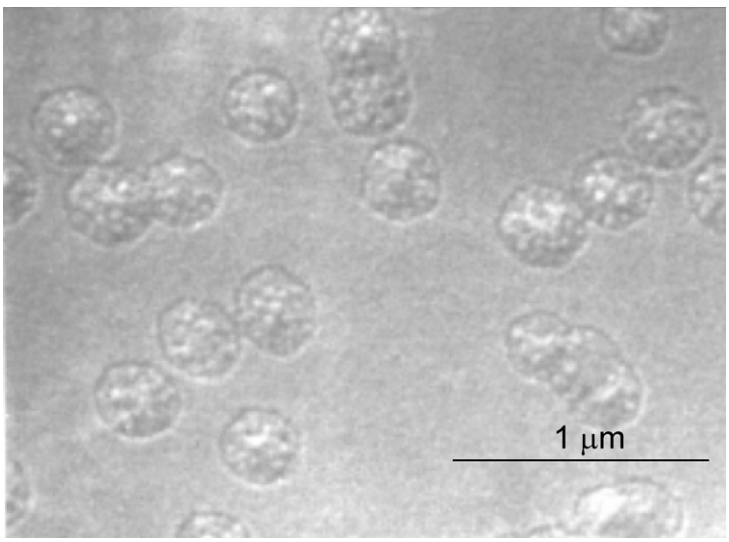

Fig. 6. SEM micrograph of as-deposited PLZT film showing nano-crystals forming in an amorphous matrix.

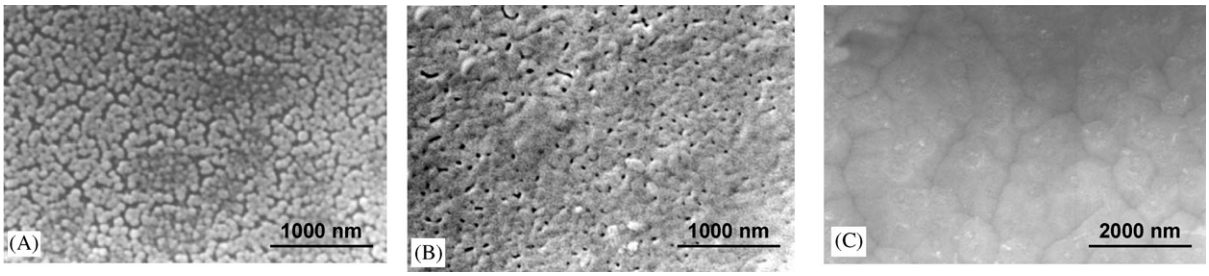

Fig. 7. SEM micrographs of PLZT films annealed by (a) RTA at 550°C for 2 min, (b) RTA at 800°C for 2 min, and (c) furnace annealing at 700°C for 30 min.

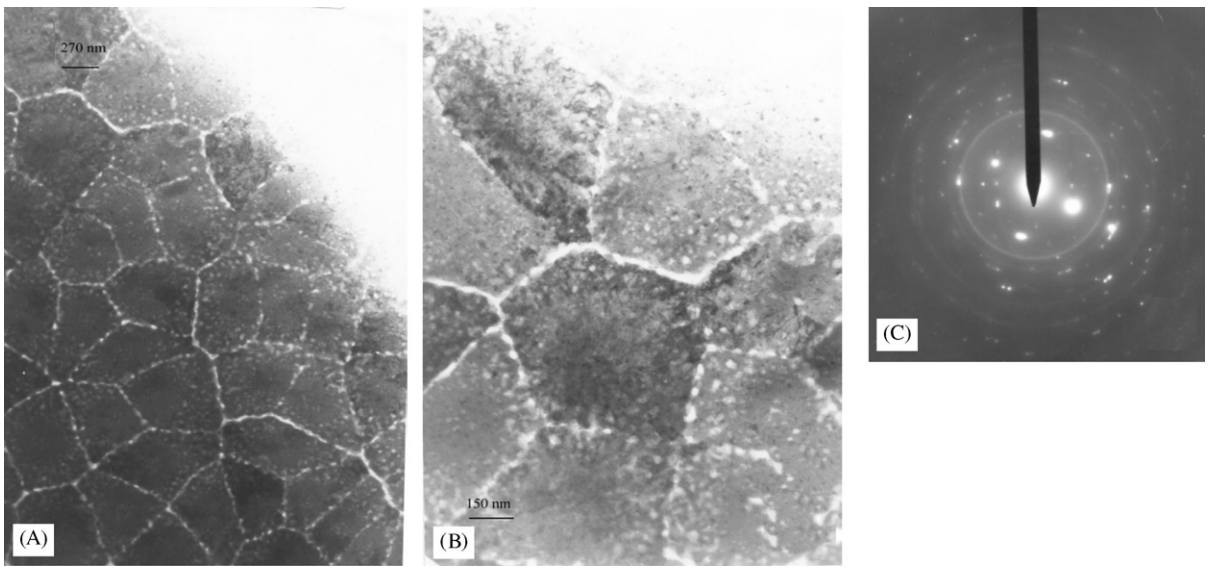

Fig. 8. TEM images (a and b) and the selected area diffraction pattern (c) of post-RTA films exhibiting a microporous equiaxed polycrystalline grain structure.

temperature differential across our samples (center-to-edge) is probably less than 1°C due to their small size (10 mm × 10 mm). It can also be assumed that samples reached steady-state in our RTA tests since our RTA holding time was always longer than 10 s. The ramp-up time was around 20 s for RTA temperatures 700–730°C. In steady-state condition after the ramp-up, a high gas flow-rate can reduce the wafer sample temperature and also cause temperature nonuniformity. Therefore, a low flow-rate (<10 scfh) was used in this study. A low cooling rate (10°C/min) was essential to eliminate film cracking caused by thermal stresses due to thermal expansion mismatch of the PLZT film and the substrate.

The microstructure of films were polycrystalline perovskite with a small amount of pyrochlore after RTA processing. Selected area diffraction revealed a fairly random polycrystalline structure as seen in Fig. 8. The perovskite phase was determined to possess a tetragonal distortion with lattice constants $a = 0.4086$ nm and $c = 0.4109$ nm as evaluated from X-ray diffraction [9]. The SAD rings reflect the existence of a secondary phase in the film as pyrochlore as shown. Equiaxed grains are randomly distributed with porosity clearly seen at the grain boundaries and peripheries of some grains (Fig. 8). The existence of such porosity and grain shapes are similar to those reported for sol–gel derived PZT films [10] and chemical solution deposited PLZT films on platinized silicon [11]. A good discussion of the kinetics of the perovskite transformation during RTA of sputtered PZT was reported by Hu et al. [12].

Films that were furnace annealed at 700°C from 20 min to 1 h revealed splitting of perovskite phase into a pair of plates (Fig. 9). The average size of such a split precipitate was 35 nm in width and 150 nm in length.

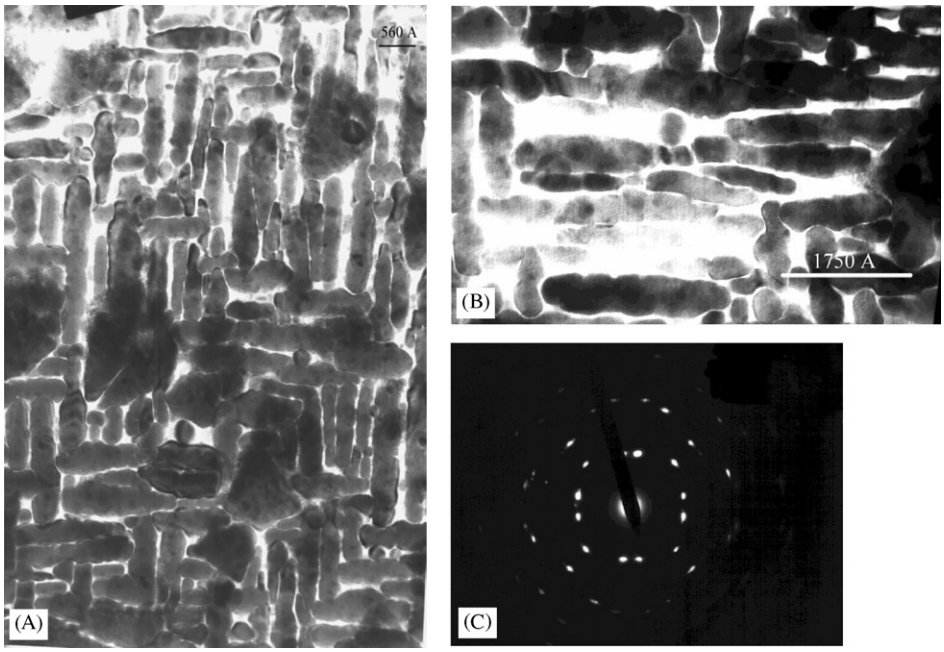

Fig. 9. TEM images (a and b) and selected area diffraction pattern (c) of a furnace annealed PLZT film on sapphire with a single-phase perovskite exhibiting elongated paired-plates.

These films were sputter-deposited at a high temperature, 490°C at which interfacial energy anisotropy is expected to be small. In this case, the film orientation was determined by X-ray diffraction and only (1 1 0) and strong (2 0 0) perovskite peaks were observed in the as-deposited film. The annealed film was strongly (1 1 0) oriented with a much weaker (2 0 0) component, which suggest a rotation in the plane during the transformation. The transformed cubic particle which splits then belongs to the stable (1 1 0, 1 $\bar{1}$ 0) family in perpendicular directions in orientation. The initial growth process requires cross-sectional microscopy to identify the intermediate The growth of (1 1 1) oriented sputtered PLZT (9/65/35) films with a random grain orientation and an average grain size of 300 nm were reported on PLT buffered c-sapphire substrates [13]. The PLZT (9/65/35) films on r-sapphire in this study which were furnace annealed exhibited a cubic structure with a lattice constant of 0.409 nm. The lattice mismatch between the PLZT film with perovskite phase and the sapphire substrate is significant, approximately 6% [14], to generate internal stresses which can be compounded by the additional thermal stresses during the cooling cycle of annealing. The PLZT has an average coefficient of thermal expansion (CTE) of $5.4 \times 10^{-6}\,°C^{-1}$ that is smaller than the CTE of r-sapphire substrate, 5.8–$7.7 \times 10^{-6}\,°C^{-1}$, in the temperature range of 20–500°C. Thus, we anticipate that a two-dimensional compressive stress is imparted on the PLZT thin film deposited on sapphire as the substrate contracts more than the film upon cooling down to room temperature. It is thought that a high deposition temperature of 490°C leads to homogeneous formation of single-phase perovskite under internal stress and upon annealing the splitting process becomes visible. However, previous results by others on PLZT (9/65/35) films on c-sapphire have not shown any paired plate formation [13]. The orientation of films were of (1 1 1) which is different than the film orientation observed (1 1 0) on r-sapphire substrates in this study. This may suggest that the film orientation is playing a more important role than the thermal mismatch between the film and the substrate.

Alternatively, it may also be possible to explain this type of structure by formation of 90° domains due to relative coherency strain generated during the cooling cycle as reported by Foster et al. [15] on epitaxial $PbTiO_3$ thin films on various substrates. Dielectric measurements on PLZT films [16] of this study which were reported earlier indicated that the furnace annealed quasi-cubic films exhibit a Curie temperature of approximately 137°C, while those of RTA were somewhat smaller ~120°C with a tetragonal phase. This indicates that strain relaxation kinetics after phase transformation of these films is expected to play an important role in formation of grains and such modulated structures. Faster cooling rates may have hindered the formation of domain patterns as in RTA films as compared FA films in this case due to reduced

mobility of point defects (e.g. oxygen vacancies) as suggested by Foster et al. [15].

A strong correlation exists between microstructure development and the processing conditions of PLZT thin films on r-sapphire. The pyrochlore that forms at deposition temperatures of 300°C usually has a crystallite size of 20–30 nm while the perovskite phase crystallite size is larger, 60 nm, at its first nucleation approximately at around deposition temperature of 460°C. After an annealing procedure, a predominant perovskite phase results with usually an equiaxed grain morphology with a somewhat larger grain size. However, the dielectric properties are quite different with higher values resulting from furnace annealed films compared to those from post-RTA films [16].

5. Summary and conclusion

A complex microstructure results in PLZT thin films on sapphire depending on deposition and annealing conditions. Precipitate splitting (or pair-plate formation) was observed only in PLZT films on sapphire that were deposited at high temperatures, >490°C, after furnace annealing. It is possible that this is related to the internal stress in the films due to both lattice mismatch and the CTE differential between the film and the substrate. However, it is more likely that the film lattice mismatch and substrate orientation play a more significant role in paired plate formation than the thermal expansion mismatch. Further evaluation of cross-sectional TEM of as-deposited and annealed films will help understanding the possible domain formation, the nucleation and the growth process of these paired plates.

Acknowledgements

This work was supported by TRW subcontract GZ30602W35 Ultra Program under DARPA prime contract DAAH 04-93-G-00029.

References

[1] Krishnakumar S, Ozguz VH, Fan C, Cozzolino C, Esener SC, Lee SH. IEEE Trans Ultrasonics Ferroelectrics Freq Control 1991;38:585.
[2] Hwang YS, Paek SH, Lee JH, Park CS, Choi JS, Jung JK, Kim YN. J Mater Sci: Mater Electron 1996;7:309.
[3] Yoshikawa Y, Suzuki KT. J Am Ceram Soc 1990;73:31.
[4] Tani T, Payne DA. J Am Ceram Soc 1994;77:1242.
[5] Miyazaki T, Imamura H, Kozakai T. Mater Sci Eng 1982;54:9.
[6] Maheshwari A, Ardell AJ. Scr Metall Mater 1992;26:374.
[7] Li DY, Chen LQ. Acta Mater 1999;47:247.
[8] Lin YT, Subrahmanyan R, Sitaram AR, Orlowski M. Mater Res Soc Symp Proc 1993;303:231.
[9] Tunaboylu B, Harvey P, Esener SC. Integ Ferroelectrics 1998;19:11.
[10] Hsueh CC, MeCartney ML. J Mater Res 1991;6:2208.
[11] Cross JS, Fujiki M, Tsukada M, Kotaka Y, Goto Y. J Mater Res 1999;14:4366.
[12] Hu H, Peng CJ, Krupanidhi SB. Thin Solid Films 1993;223:327.
[13] Wasa K, Satoh T, Tabata K, Adachi H, Yabuuchi Y, Setune K. J Mater Res 1994;9:2960.
[14] Lee WE, Lagerlof KPD. J Electron Microsc Tech 1985;2:247.
[15] Foster CM, Pompe W, Daykin AC, Speck JS. J Appl Phys 1996;79(3):1405.
[16] Tunaboylu B, Harvey P, Esener SC. IEEE Trans Ultrasononics Ferroelectrics Freq Control 1998;45:1105.
[17] Preston KD, Haertling GH. Integ Ferroelectrics 1996;1:89.